Nuclear Instruments and Methods in Physics Research A 618 (2010) 331–335

Contents lists available at ScienceDirect

Nuclear Instruments and Methods in Physics Research A

journal homepage: www.elsevier.com/locate/nima

Optimization study of a transportable neutron radiography unit based on a compact neutron generator

J.G. Fantidis, G.E. Nicolaou *, N.F. Tsagas

Laboratory of Nuclear Technology, School of Engineering, 'Democritus' University of Thrace, Xanthi, Greece

ARTICLE INFO

Article history:
Received 16 December 2009
Received in revised form
16 February 2010
Accepted 16 February 2010
Available online 26 February 2010

Keywords:
Fast neutron radiography
Thermal neutron radiography
MCNP
RoHS Directive

ABSTRACT

A transportable fast and thermal neutron radiography system, incorporating a compact DD neutron generator, has been simulated using the MCNPX code. The materials considered were compatible with the European Union Directive on 'Restriction of Hazardous Substances'(RoHS) 2002/95/EC, hence excluding the use of cadmium and lead. Appropriate collimators were simulated for each of the radiography modes. With suitable aperture and collimator designs, it was possible to optimize the parameters for both fast and thermal neutron radiographies, for a wide range of values of the collimator ratio. The system simulated allows different object sizes to be studied with a wide range of radiography parameters.

© 2010 Elsevier B.V. All rights reserved.

1. Introduction

Neutron radiography (NR) has been established as a testing technique and as a research tool for over 60 years [5,19,1,10]. During this time, NR has evolved in use and applications, issues still growing while the quality and the prospectives of the various techniques are continuously improving [20]. The technique is widely used in security applications, engineering studies and industry in order to determine structural defects, in geology, medicine and biological research [12,18].

In particular, thermal neutron radiography, as opposed to fast neutron radiography, has been thoroughly developed and is commercially available. This stems from the availability of high-intensity thermal neutron beams from nuclear research reactors and neutron sources [7]. However, their use is basically limited to relatively thin objects. The use of high energy neutrons for radiography purposes can be of great benefit when bulky objects have to be investigated. Fast neutron radiography with neutron energies greater than 1 MeV could open up a new range of possibilities for non-destructive inspections. In comparison with thermal neutrons, there is little variation in attenuation among the elements when neutron energies are in the MeV range [17]. However, the number of nuclei per unit volume does vary from element to element, and penetration of fast neutrons through most materials is quite good. This makes them a unique tool for non-destructive quality inspection in production and service of large-scale objects and products containing light and heavy elements simultaneously.

In this work, a transportable unit for thermal and fast radiography, incorporating a deuterium–deuterium (DD) neutron generator, has been simulated using the MCNPX Monte Carlo code [15]. A transportable unit would offer the possibility of enlarging the range of applications of both thermal and fast NR. The aim of the work is to design a unit optimized in terms of the moderator, collimator and shielding when in use, rendering it suitable for quality non-destructive testing, while ensuring adequate occupational radiation protection measures. The proposed unit is designed according to article 4 of the RoHS Directive 2002/95/EC, regarding the choice of materials. Hence, lead, mercury, cadmium, hexavalent chromium, polybrominated biphenyls and polybrominated diphenyl ethers have been excluded from the design [4].

2. The radiography unit

The unit is designed in the form of two coaxial cylinders connected at one end which is open (Fig. 1). The left-hand side cylinder has a length and a radius of 440 and 90 cm, respectively, while the other is 248 cm long with a radius of 108 cm. The walls of the cylinders are made of polyethylene with 5% boron (PE-B) covered by bismuth (Bi) on the outside. In the case of the former cylinder, the thicknesses of the PE-B and Bi are 57.5 and 2.5 cm, respectively. In the case of the right-hand side cylinder, these dimensions are 47 and 1 cm, respectively. The left-hand side cylinder houses, towards its open end, an imaging neutron collimator of variable length and next to it the neutron

* Corresponding author.
E-mail address: nicolaou@ee.duth.gr (G.E. Nicolaou).

0168-9002/$ - see front matter © 2010 Elsevier B.V. All rights reserved.
doi:10.1016/j.nima.2010.02.107

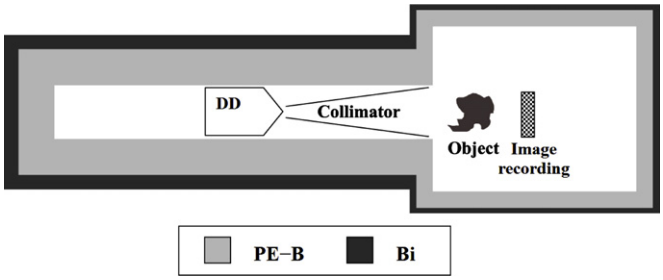

Fig. 1. Side view of the geometric configuration of the irradiating system (not in scale).

generator. The object under examination is placed, together with the image recording apparatus, within the other cylinder.

2.1. The neutron generator

A number of candidate neutron sources for fast and thermal neutron radiography could be considered. Nuclear reactors would provide high intensity neutron beams but are expensive, non-portable and have limited facilities (availability and location). Isotopic neutron sources, such as ^{241}Am/Be and ^{252}Cf, although suitable for both in-situ fast and thermal radiography, emit a low intensity of neutrons with energies up to 10 MeV, which would require adequate shielding.

The DD neutron generators seem to be an attractive choice because they produce neutrons, with an energy approximately equal to 2.5 MeV, suitable for both thermal and fast radiography. Furthermore, they offer an on/of switching of the emitted neutrons. They have a compact size and a relatively high neutron flux. In this work, a coaxial RF-plasma DD neutron generator was simulated [22,16]. It is the most powerful portable neutron generator and capable of delivering 10^{11} n s^{-1}. The unit has overall dimensions of 60 cm × 45 cm, with an extraction aperture composed from seven slits 1.5 mm wide and 75 mm in height.

2.2. Thermal neutron collimator

The collimator ratio (L/D), which determines the quality of the NR imaging for a given design of the collimator, is given by the following equations:

$$\phi_i = \frac{\phi_\alpha}{16(L_S/D)^2} \tag{1}$$

and

$$u_g = L_f \frac{D}{L_s} \tag{2}$$

where L_f is the image surface to object distance, L_s the source to object distance, D the inlet aperture diameter, φ_i the neutron flux at the image plane, φ_α the neutron flux at the aperture and u_g the geometric unsharpness.

The beam divergence, a significant measure of the usefulness of the beam near its periphery, is described by its half-angle (θ) given by [5]

$$\theta = \tan^{-1}\left(\frac{I}{2L}\right) \tag{3}$$

where I and L are the maximum dimensions of the image area and the length of the collimator. The imaging quality of a system is further characterized by the thermal neutron content (TNC), describing the number of thermal neutrons within the neutron beam

$$\text{TNC} = \frac{\text{thermal neutron flux}}{\text{total neutron flux}} \tag{4}$$

and the relative intensities of the neutron (n) and the photon (γ) components of the beam, with (n/γ) typically greater than 10^4 n cm^{-2} mSv^{-1} [8].

In the case of thermal NR, the choice of the moderator needed to thermalise the neutrons emitted by the source is the first step in the design of the unit. The moderator should provide the largest possible flux of thermal neutrons extracted by the collimator towards the object. The material sought should thermalise the neutrons in a small number of collisions, while not absorbing them to a great extent. Fig. 2 shows the proposed collimator system for thermal neutron radiography.

In this context, the 2.5 MeV fast neutrons from the generator are thermalised using 2.1 cm thick high density polyethylene (HD-PE) (1). Hence, a maximum thermal neutron flux at the collimator inlet aperture is achieved. The collimator being modelled is made of two parts. The first, which is an HD-PE cylinder (2), with a radius of 8 cm and length of 14 cm, incorporates a conic collimator either made of single sapphire or that is void. The conic collimator has a length of 14 cm and radii 3.75 and 0.5 cm, with the larger radius close to the source. The single sapphire (Al_2O_3) is commonly used for fast neutron filtration [21,14].

Next to the HD-PE cylinder, a divergent collimator is situated, which determines to a great extent the quality of the image for a given source type. The material used in the design of the collimator should prevent stray and scattered neutrons from reaching the object through absorbing them, hence improving the unsharpness of the image obtained. In this respect, the inner lining of the collimator is particularly important and it should be made of a neutron-absorbing material [5]. The lining is composed of a 0.8 cm layer of boral covered by PE-B with a depth of 3.2 cm as a shielding against stray neutrons. Bismuth (Bi) with 1 cm of thickness was chosen as the collimator casing.

2.3. Fast neutron collimator

The quality of fast NR imaging is determined by the collimator ratio (L/D) in a similar way as in the case of thermal NR. The considerable penetration of fast neutrons inside an object results in a geometric unsharpness u_g given by the equation [2]

$$u_g = \frac{Dt}{L-t} \tag{5}$$

where t is the image surface to object distance, L the distance from the aperture to the image plane and D the collimator aperture diameter.

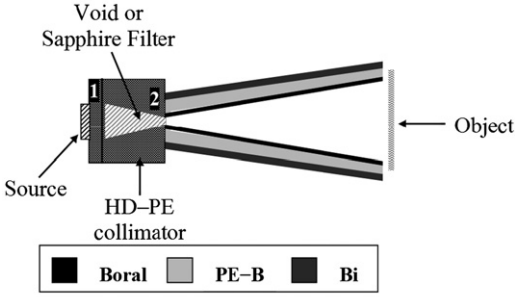

Fig. 2. The collimator geometry for thermal neutron radiography with the sapphire filter in front of the collimator (not in scale).

The imaging quality of a fast neutron radiography facility would be further characterized by the beam quality profile, described by the number of uncollided neutrons that reach the detector position within the neutron beam.

Collimation of fast neutrons is not as straightforward as in the case of thermal neutrons. This is due to the lack of sufficiently strong absorbers for fast neutrons, which are needed to construct apertures or collimator walls. Nevertheless, fast neutron imaging systems can be effectively built and used. The lack of such materials results in neutrons emerging from the walls of a collimator. Some of these re-merging neutrons can scatter towards the area of exposure projected by the collimator on the object. Scattering from the collimator walls would also produce slower neutrons downgrading the quality of the extracted beam, which ideally should have the same energy distribution as that of the source (uncollided neutrons). Furthermore, the neutron moderating materials traditionally used are also scattering materials deteriorating the quality of the beam profile. Therefore, metals are found to be more suitable as collimator material for fast neutrons. Then, neutrons would be scattered away from the interior walls of a collimator following very few collisions, with an insignificant loss in energy. Hence, iron and tungsten are preferred as collimator materials, with the former being cheaper and easier to fabricate [9].

The fast neutron collimator, considered in this work, comprises two parts (Fig. 3). The first is a conic convergent one, with a length of 14 cm and radii of 3.75 and 0.5 cm, inside a PE-B cylinder with a radius of 8 cm. The second collimator is a divergent one, with an inlet aperture of 1 cm, and a variable length and walls made of 4 layers of different materials. These materials from the inside outwards are 7 cm thick iron (Fe), 0.5 cm thick gadolinium (Gd), 2 cm thick PE-B and 1.5 cm Bi.

This first collimator is capable of absorbing some scattered neutrons and restricting their energy and population towards the second collimator, thus improving the quality of the beam profile. The aperture, situated between the two parts, is a combination of two materials: 0.3 and 1 cm-thick layers of Gd and Bi used to absorb thermal neutrons while preventing the gamma rays generated within the other materials from reaching the second collimator. Furthermore, there is a 2 cm thick layer of Bi covering the front side of the collimator. The object-to-detector distance controls the recording of scattered neutrons, which affect the imaging contrast and decrease by $1/t^2$.

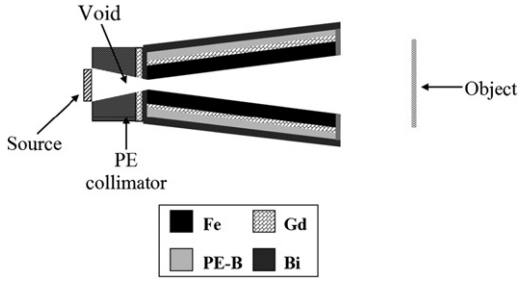

Fig. 3. The aperture geometry and the collimator for fast neutron radiography (not in scale).

3. Results and discussion

The system was designed under the constraint that the dose equivalent rate (DER) would remain below the annual occupational dose limit of 0.05 Sv (or 25 μSv h^{-1}) at the external surface of the shielding of the neutron generator. The total dose rate, due to the neutrons and photons, was calculated with the MCNPX Monte Carlo code, using the F2, Fm2 tallies and the DE, DF cards. The F tallies describe the neutron flux on a surface, while the D cards convert the absorbed dose to equivalent dose. Calculations were performed for a total number of histories per starting neutron (NPS) of 2×10^8 yielding an accuracy of $<1\%$ in the calculations. The maximum resulting total DER is 14.8 μSv h^{-1} and occurs at positions closest to the source. The total dose comprises the neutrons and the photons, the latter from the interaction of the neutrons and the PE-B moderator material. The values of the DER are 7.5 and 7.3 μSv h^{-1}, respectively. Hence, the dimensions and materials chosen under the RoHS directive render a unit with an overall weight of 23,800 kg, which satisfies the occupational dose limit constraints.

In the case of thermal neutron radiography, the proposed system comprises a collimator with a variable collimator length (L=50–150 cm), diameter of its aperture next to the image plane (D_0=12–20 cm) and divergence angle (θ) of the beam (θ=3.8–6.8°), while the inlet aperture (D) of the collimator is 1 cm. The distance between the object and the imaging detector (L_f) was considered to be 0.5 cm [5]. The variation of the thermal neutron flux at the field of view at the object position was less than 1.5%.

The calculated thermal neutron flux (f_{th}), TNC and (n/γ) parameters are shown in Table 1 for different collimator parameters, with and without the single sapphire filter. The neutron flux was calculated with the aid of the MCNPX code using the F2 tally, which gives the required neutron flux averaged over a surface in neutrons cm^{-2} per starting neutron. Calculations were carried out with NPS$=3\times10^7$ neutrons, yielding an accuracy $<0.5\%$. An energy boundary of 0.01–0.3 eV was used to score the thermal neutron flux. The gamma dose, in the ratio n/γ, was calculated with the F2, Fm2 tallies and the DE, DF cards. These calculations were performed for NPS$=6\times10^8$ neutrons, yielding an accuracy of $<2\%$ in the calculations. According to Table 1, the (n/γ) parameter remains, in all circumstances, higher than the recommended limit of 10^4 n cm^{-2} mSv^{-1}, ranging between 6.5×10^4 and 1.3×10^6 n cm^{-2} mSv^{-1}.

The f_{th}, TNC and (n/γ) parameters were determined for different sapphire filter thicknesses in the case of three L/D values

Table 1
The thermal NR calculated parameters using the proposed system.

L (cm)	L/D	D_0 (cm)	U_g (cm)	Thermal NR calculated parameters without sapphire filter			Thermal NR calculated parameters with 14 cm sapphire filter		
				f_{th} (n cm^{-2} s^{-1})	TNC (%)	n/γ (n cm^{-2} mSv^{-1})	f_{th} (n cm^{-2} s^{-1})	TNC (%)	n/γ (n cm^{-2} mSv^{-1})
50	50	12	1.00E−2	1.58E+04	3.57	7.01E+5	9.66E+03	27.06	6.47E+4
75	75	14	6.67E−3	7.20E+03	3.77	8.75E+5	4.40E+03	31.45	7.03E+4
100	100	16	5.00E−3	4.12E+03	3.89	9.17E+5	2.52E+03	33.95	7.75E+4
125	125	18	4.00E−3	2.62E+03	3.88	1.24E+6	1.60E+03	34.45	8.41E+4
150	150	20	3.33E−3	1.81E+03	3.90	1.32E+6	1.11E+03	35.36	9.73E+4

Table 2
The thermal NR calculated parameters for three L/D values with variable sapphire filter length.

Sapphire filter (cm)	$L/D=50$			$L/D=100$			$L/D=150$		
	f_{th} (n cm^{-2} s^{-1})	TNC (%)	n/γ (n cm^{-2} mSv^{-1})	f_{th} (n cm^{-2} s^{-1})	TNC (%)	n/γ (n cm^{-2} mSv^{-1})	f_{th} (n cm^{-2} s^{-1})	TNC (%)	n/γ (n cm^{-2} mSv^{-1})
0	1.58E+4	3.57	7.01E+5	4.12E+3	3.89	1.01E+6	1.81E+3	3.90	1.32E+6
1	1.53E+4	4.14	5.92E+5	3.99E+3	4.52	8.47E+5	1.75E+3	4.65	1.08E+6
2	1.47E+4	4.61	5.16E+5	3.84E+3	5.40	6.87E+5	1.69E+3	5.53	8.76E+5
3	1.41E+4	5.63	4.10E+5	3.69E+3	6.47	5.54E+5	1.62E+3	6.64	7.06E+5
4	1.36E+4	6.71	3.33E+5	3.54E+3	7.65	4.52E+5	1.55E+3	7.89	5.73E+5
5	1.30E+4	7.88	2.74E+5	3.39E+3	9.14	3.65E+5	1.49E+3	9.36	4.66E+5
6	1.26E+4	9.59	2.20E+5	3.28E+3	10.60	3.06E+5	1.44E+3	11.24	3.78E+5
7	1.21E+4	11.34	1.81E+5	3.17E+3	13.03	2.42E+5	1.39E+3	13.37	3.09E+5
8	1.18E+4	13.56	1.48E+5	3.07E+3	15.48	1.99E+5	1.35E+3	15.57	2.59E+5
9	1.14E+4	16.02	1.23E+5	2.97E+3	18.01	1.67E+5	1.31E+3	18.59	2.11E+5
10	1.10E+4	18.46	1.04E+5	2.86E+3	21.34	1.36E+5	1.26E+3	21.36	1.78E+5
11	1.07E+4	21.32	8.82E+4	2.79E+3	24.65	1.16E+5	1.22E+3	25.39	1.47E+5
12	1.03E+4	23.67	7.75E+4	2.69E+3	28.18	9.85E+4	1.18E+3	28.70	1.26E+5
13	9.97E+3	25.84	6.93E+4	2.60E+3	30.56	8.83E+4	1.14E+3	32.83	1.07E+5
14	9.66E+3	27.06	6.47E+4	2.52E+3	33.95	7.75E+4	1.11E+3	35.36	9.73E+4

Table 3
The fast NR calculated parameters using the proposed system.

L (cm)	L/D	D_0 (cm)	θ (deg)	Fast NR calculated parameters with $t=25$ cm			Fast NR calculated parameters with $t=50$ cm		
				U_g (cm)	f_F (n cm^{-2} s^{-1})	Uncollided f_F (%)	U_g (cm)	f_F (n cm^{-2} s^{-1})	Uncollided f_F (%)
100	100	12	3.4	1.20E−1	5.80E+4	97.07	2.00E−1	3.30E+4	97.27
150	150	14	2.7	8.57E−2	3.11E+4	97.75	1.50E−1	2.00E+4	98.00
200	200	16	2.3	6.67E−2	1.94E+4	97.94	1.20E−1	1.35E+4	98.15
250	250	18	2.1	5.45E−2	1.32E+4	98.26	1.00E−1	9.72E+3	98.46
300	300	20	1.9	4.62E−2	9.57E+3	98.54	8.57E−2	7.26E+3	98.76

(Table 2). The thermal neutron flux would vary from 1.1×10^3 up to 1.6×10^4 n cm^{-2} s^{-1} for a maximum neutron yield by the generator of 10^{11} n s^{-1}. These values are somewhere lower in comparison to low power research reactors [23]. The TNC varies from 3.6% to 35.4%. Good-quality thermal neutron images require exposures of the order of 10^7 n cm^{-2} in order to detect defects smaller than 0.025 cm [6], with the exposure time being proportional to the thermal neutron flux. In the case of $L/D=50$, the exposure time is 10.5 and 17.2 min without filter and with the 14 cm single sapphire filter, respectively. Higher L/D values would require higher exposure times but offer radiographies with better quality [19] in the cases of $L/D=100$ and 150, exposure times in the range 0.67–1.1 and 1.53–2.51 h would be required, respectively. In this case, neutron imaging plates (or X-ray films with converter) seem to be a better choice [11].

The suggested unit was further simulated with MCNPX code for fast neutron radiography making use of the fact that the DD neutron generator is a strong fast neutron emitter. Fast neutron fluxes (f_F) were calculated using the F2 tally with NPS$=5\times10^7$ neutrons, yielding an accuracy $<0.5\%$ (Table 3). The system has been considered with a second collimator having variable length ($L=100$–300 cm), diameter of its aperture next to the image plane ($D_0=12$–20 cm), a divergence angle (θ) of the beam ($\theta=1.9$–3.4°). The object–detector distance (t) was considered to be 25 or 50 cm. The distance between the end of the collimator and the detector was $2t$. The collimator weight varies between 450 and 1340 kg. The n/γ ratio is higher than 10^{11} n cm^{-2} mSv^{-1}. This is due to the absence of the HD-PE moderator, which has reduced considerably the photons within the system while increasing the fast neutron component.

The calculated parameters for the fast neutron radiography system are shown in Table 3. The uncollided fast neutron flux, which characterizes the beam quality, ranges between 97.1% and 98.5% for $t=25$ cm and between 97.3% and 98.8% for $t=50$ cm. The fast neutron flux varies from 7.3×10^3 to 5.8×10^4 n cm^{-2} s^{-1}. The fast neutron flux at the field of view at the object was uniform to within 1%. Except from the fast neutron flux, the calculated parameters have values comparable with low power research reactors [3]. The detection of defects 0.1 cm in size would require an exposure of about 1.5×10^7 fast neutron cm^{-2} [13], with the exposure time being analogous to the fast neutron flux. In the case of $L/D=100$, the exposure time is 4.3 and 7.6 min, with $t=25$ and 50 cm, respectively. Higher L/D values would entail higher exposure times: for example $L/D=200$ and 300 necessitate exposure times in the range 12.9–18.5 and 26.1–34.4 min, respectively. An imaging system based on a CCD-detector is suitable for visualising fast neutron fields [13].

4. Conclusions

A transportable system using a DD compact neutron generator has been simulated, for radiography purposes, using the MCNPX Monte Carlo code. All the materials considered were chosen according to the EU Directive 2002/95/EC, excluding lead and cadmium. Hence, bismuth was used in order to replace the lead, while boral or gadolinium was used to replace the cadmium. Appropriate collimators have been simulated for fast and thermal neutron radiography. The use of sapphire in the thermal neutron collimator has led to improved parameters associated with NR. According to the results obtained, the proposed system has dimensions that render it suitable for transportation with a medium-sized lorry. The simulated facility has a wide range of values for the parameters characterising the thermal and fast neutron radiographies, resulting in radiographs of variable quality.

References

[1] J. Bahnart, Advanced Tomographic Methods in Materials Research and Engineering, Oxford University Press, Oxford, 2008.
[2] H. Berger, F. Iddings, Neutron Radiography, A State-of-the-Art Report, Nondestuctive Testing Information Analysis Center, 1998.
[3] T. Bücherl, E. Kutlar, C.L.V. Gostomski, E. Calzada, G. Pfister, D. Koch, Appl. Radiat. Isot. 61 (2004) 537.
[4] B. D'Mellow, D.J. Thomas, M.J. Joyce, P. Kolkowski, N.J. Roberts, S.D. Monk, Nucl. Instr. and Meth. Phys. Res. A 577 (2007) 690.
[5] J.C. Domanus, Collimators for Thermal Neutron Radiography—An Overview, D. Reidel Publishing Company, 1987.
[6] K. Gibbs, H. Berger, T. Jones, D. Polansky, J. Haskins, D. Schneberk, J. Brenizer, in: ASNT Fall Conference, October 1999.
[7] S. Glasstone, Principles of Nuclear Reactor Engineering, Macmillan and Company Ltd, 1970.
[8] M.R. Hawkesworth, At. Energy Rev. 15 (1977) 169.
[9] E.M.A. Hussein, Handbook on Radiation Probing, Gauging, Imaging and Analysis, Volume II: Applications and Design, Kluwer Academic Publishers, 2004.
[10] E. Lehmann, N. Kardjilov, in: J. Banhart (Ed.), Advanced Tomographic Methods in Materials Research and Engineering, Oxford University Press, Oxford, 2008.
[11] E.H. Lehmann, P. Vontobel, G. Frei, C. Bronnimann, Nucl. Instr. and Meth. 531 (2004) 228.
[12] W.J. Lewis, L.G.I. Bennett, T.R. Chalovick, O. Francescone, in: Proceedings of the 15th World Conference on Nondestructive Testing, Rome, Italy, October 15–21, 2000.
[13] V. Mikerov, W. Waschkowski, Nucl. Instr. and Meth. 424 (1999) 48.
[14] D.F.R. Mildner, G.P. Lamaze, J. Appl. Crysallogr. 31 (1998) 835.
[15] D.B. Pelowitz, MCNPXTM User's Manual Version 2.5.0, 2005.
[16] J. Reijonen, F. Gicquel, S.K. Hahto, M. King, T.P. Lou, K.N. Leung, Appl. Radiat. Isot. 63 (2005) 757.
[17] A.R. Spowart, J. Phys. E: Sci. Instrum. 5 (1972) 497.
[18] M.A. Stanojev Pereira, F. Pugliesi, R. Pugliesi, Braz. J. Phys. 38 (3A) (2008) 346.
[19] B. Schillinger, E. Lehmann, P. Vontobel, Physica B 276 (2000) 59.
[20] M. Strobl, N. Kardjilov, A. Hilger, I. Manke, J. Banhart, Physica D 42 (2009) 243001.
[21] D.C. Tennant, Rev. Sci. Instrum. 2 (1988) 59.
[22] 〈www.adelphitech.com〉.
[23] M. Zawisky, F. Hameed, E. Dyrnjaja, J. Springer, Nucl. Instr. and Meth. A 587 (2008) 342.